Evolution of metallicity gradients in Milky Way analogues using EAGLE simulations.

Trabajo de fin de grado.
Sección de ciencias. Facultad de física.

July, 2018

Author:
Aridai Bordón Sánchez

Supervisors:
Dr. Christopher Brook
Dr. Claudio Dalla Vecchia

Soy hombre,
duro poco y larga es la noche
pero miro a las estrellas.

Octavio Paz (1914 - 1998)

Contents

Abstract

En los últimos años ha habido un creciente intéres en el estudio de la evolución química de galaxias. En estos trabajos encontramos numerosos autores que defienden que la metalicidad juega un importante rol en procesos de formación y evolución galácticos.

En este documento se ha analizado el papel de la metalicidad en distintas muestras de galaxias (centrándonos en aquellas con propiedades similares a la Vía Láctea) de z=0 a z=1.5 y su relación con el resto de propiedades.

Todos los datos han sido obtenidos gracias al lanzamiento público de las simulaciones hidrodinámicas EAGLE. En la inmensa mayoría del trabajo hemos usado como referencia la simulación RefL0025N0752 que otorga la mayor resolución aunque, cómo mostraremos más adelante, incluso esta resolución es insuficiente para dar cuenta de algunos resultados observacionales.

Una de las principales dificultades ha sido identificar galaxias similares a la Vía Láctea (MW) y rastrearlas a tráves de los distintos redshifts dados por la simulación. Se ha solucionado el primer problema estableciendo límites a propiedades clave de las galaxias como su masa, su morfología, su ratio de formación de estrellas o la última vez que ha sufrido un gran merger. Finalmente hemos obtenido una muestra total de 24 galaxias en el intervalo de masas requerido de las cuáles 3 cumplen el resto de requisitos impuestos para la Vía Láctea.

El rastreo se ha llevado a cabo usando la herramienta dada por EAGLE que permite seguir la relación entre una galaxia y todos sus descendentes además de una descripción completa de todos los merger que esta ha sufrido.

A continuación mostramos un breve resumen de los principales tópicos tratados en este documento:

Objetivos: *En este trabajo estudiamos la evolución de la metalicidad radial en distintas muestras de galaxias desde z=0 a z=1.5 usando las simulaciones hidrodinámicas ofrecida por EAGLE. Hemos puesto especial enfásis en el estudio de las propiedades capaces de caracterizar la evolución química de las galaxias como la metalicidad.*

Método: *Hemos escogido una muestra de galaxias en el intervalo de masas de la Vía Láctea clasificándolas atendiendo a sus distintas propiedades (Clasificaciones por morfología, por masa, por tiempo transcurrido desde el último*

merger, etc).

Se ha representado la evolución de características generales de la muestra de galaxias y como varían las propiedades de la muestra Vía Láctea respecto a las del resto de galaxias.

Finalmente, se ha mostrado en diagramas radiales y verticales el estado de la metalicidad a redshift 0 y su evolución desde redshift 1.5.

Resultados: *Hemos encontrado una fuerte correlación entre la morfología de las galaxias y la última vez que estas han sufrido un merger con una galaxia de al menos el 10 por ciento de su masa y distintas imágenes de la muestra de galaxias MW que indican un módelo de crecimiento inside-out.*

Además, se ha analizado la metalicidad radial y vertical a redshift 0 y 1.5.

Conclusiones: *Se ha mostrado como en las simulaciones EAGLE la metalicidad está fuertemente ligada a la "merger history" de las galaxias. Asimismo, las galaxias con mergers anteriores a redshift 1.5 muestran un crecimiento acorde a los esperado por un modelo inside-out.*

Durante el análisis de la metalicidad radial encontramos como el comportamiento de la muestra de galaxias MW se asemeja a la muestra de galaxias que no ha sufrido un gran merger al menos desde z=1.5.

También mostramos como el gradiente de metalicidad es menor para galaxias que han sufrido un proceso de merger recientemente y que el tiempo desde el último merger es un parámetro fundamental que determina la distribución de metalicidad radial.

Finalmente, hemos mostrado como la simulación EAGLE es incapaz de diferenciar el disco grueso del disco fino usando la metalicidad vertical a diferencia de lo que muestran distintas observaciones en nuestra propia galaxia (e. g Marsakov and Borkova (2008) [16]).

Acknowledgements

I would like to thanks my two supervisor Claudio Dalla Vecchia and, specially, Chris Brook for all their continuous monitoring and support during the elaboration of the present paper.

Also, I acknowledge the Virgo Consortium for making their simulation data available. The EAGLE simulations were performed using the DiRAC-2 facility at Durham, managed by the ICC, and the PRACE facility Curie based in France at TGCC, CEA, Bruyresle-Chtel.

Thanks also to the IAC for letting me use their computers and storage the data provided by the EAGLE simulation, to M. Bordón, Y. Ucman and J. Cabeza for their help testing the programs and to M. Crosa, J. C. Nieves and L. Pérez for their support and counsel in the presentation and style of this document.

1 Overview

The classical theory of galaxy formation was developed about 40 years ago with the initial work of Binney (1977) which discuss the collapse of galaxies. A year later Rees & Ostriker include the idea of dark matter halos within the galaxies form.

We have to wait until 1980 when Fall and Efstathiou [7] present the standard picture about the formation of disk galaxies that state that primal disk galaxies were formed by a cloud of hot gas surrounded by dark matter that started to cool radiatively and began to contract.

Since the emission of photons is isotropic the angular momentum associated is conserved and, due the contraction, it started to spin up and flatter until it formed a surface disk density and the amount of density trigger the star formation rate.

With this idea, Fall and Efstathiou created the known today as the standard picture of galaxy formation which state that:

- The angular momentum on disk galaxies is originated from cosmological torques.
- Baryons and dark matter acquire a similar angular momentum distribution.
- Baryons conserve their specific momentum while cooling.

This picture has undergone several revisions since its publication, yet the basis premise remains a useful description of galaxy formation and continues being a reference model.

The study of the metallicity as a parameter able to characterise the formation and evolution of galaxies can be tracked backwards until Shaver et al (1983) [29] who finds that metals are no homogeneously distributed over the Milky Way. Observations have provided a wide literature that confirms the existence of radial abundance trends in disk galaxies (e.g Carrera et al (2008) [3], Kewly et al (2010) [10], Sánchez-Blázquez et al (2011) [27]). Vertical trends also have been widely study (e.g Marsakov and Borsokova (2005) [16]).

In recent years the chemical evolution of galaxies have gained a great amount of attention and its study has provided different insights in the study of galaxy evolution. Recent works use hydrodinamical simulations that show how radial metallicity can be taken as a main parameter able to characterise different of galaxies' properties

(e.g Pilkington et al (2012) [23], Kawata et al (2017) [9]).

In this work, we have analysed the metallicity gradients in the EAGLE simulations, and their evolution. We then compare with results of other theoretical works as well as observational results and look for other properties that may be correlated with these metallicity gradients.

The work have been structured in the following way: The second chapter is dedicated to the methodology used along the work furthermore we present some characteristics of the EAGLE simulation and we present the way we have selected and tracked the galaxies at different redshifts within the simulation, the third chapter is entirely dedicated to the outlining the manner in which we analysed the simulations, in the fourth chapter we present all the results obtained during the elaboration of this document and finally the last chapter is dedicated to the conclusions we have extracted from our results and what are the new lines of work that require a further investigation.

2 Objectives and methodology

The main aim of this work is to verify how does the gradient of radial metallicity change depending on the redshift for simulated galaxies that are analogous to the Milky Way, sharing properties such as stellar mass and star formation rate.

The motivation is to understand better evolutionary path of disc galaxies, and in particular the Milky Way. This could help to track backwards the evolution of our own galaxy and, maybe, be fundamental on the construction of models of the evolution of galaxies.

Moreover, the study of metallicity could provide important constrains to the way simulations treats the input of energy from star formation and supernovae into the surrounding environment, a key process in disc galaxy formation. At the present state the main difference between hydrodinamical simulations is the manner in which stellar and supernova energy is returned to the surrounding gas, and a study as this could provide some clues about the issue.

The simulations used in this work are those provided by EAGLE and the selection and tracking of galaxies have been made responding to criteria establish in past works. In the next sections we describe deeper these two topics.

2.1 The EAGLE simulations

The Virgo consortium's **E**volution and **A**ssembly of **G**a**L**axies and their **E**nvironments (EAGLE) are a series of hydrodinamical simulations that adopted the cosmological parameters provided by the Planck Collaboration ($\Omega_m = 0.307$, $\Omega_\Lambda = 0.693$, $\Omega_b = 0.04825$, $h = 0.6777$, $\sigma_8 = 0.8288$, $n_s = 0.9611$, $Y = 0.248$). Here we provide the salient aspects of the codes, and refer the reader to these papers for full detail [5, 28].

In this work the relevant simulation used is RefL0025N0752. However, during the process of testing the programs we have also used the RefL0012N0188 and RefL0100-N1504. In the following table we provide some properties of the simulations.

The high and intermediate resolution is referred to the mass of the particles, with lower mass being higher resolution. Associated to this, there is a softening length of 0.35 kpc for the high resolution and 0.70 kpc for the intermediate resolution.

Modelling a population of stars using point like particles breaks down when the

Name	Resolution	L (cMpc)	N	m_g ($M_\odot$)	m_{dm} ($M_\odot$)
RefL0025N0752	High	25	752^3	2.26 x 10^5	1.21 x 10^6
RefL0100N1504	Intermediate	100	1504^3	1.81 x 10^6	9.70 x 10^6
RefL0012N0188	Intermediate	12	188^3	—	—

Table 1: Main parameters of the simulations used. The resolution indicates the softening length of the simulation, L is the side length in comoving Mpc , N is the number of dark matter particles, whilst m_g (m_dm) is the mass of each gas (dark matter) particle.

separation of particles becomes small, with the force law unphysically diverging. To prevent the effects of such a numerical issue, gravity is 'softened' within a certain length, known as the softening length. The appropriate size of this 'softening length', and the effects on results, were explored in detail in Power et al. 2003. Usually it is taken as valid all the information beyond three times the softening lenght. For this reason in the following discussions we should only take as valid the information that is at least 1 kpc from the centre.

As we can see, we justify the use of the RefL0025N0752 simulation because it has a softening length smaller than the others and making it possible to better resolve the detailed structure of the galactic discs. Nevertheless, as we would see later, this resolution may not be enough to get some fine details such as the vertical metallicity of the thin disk.

The data of EAGLE simulations is divided in two different groups: The particles database and the galaxies database. The first one contains all the information concerning the particles of the galaxies (mass, coordinates, metallicity, etc) and is divided by the kind of particle of question (gas, star, dark matter and black hole, respectively) and by snapshot (with a total of 27), each one corresponding to a given redshift. In this work we have used mainly the particle database. A brief discussion about the way it has been analysed and extracted the data will be made in the next sections.

The galaxy database contains general data of each galaxy (total mass, radius, mass centre, etc) and can be obtained directly from the EAGLE website.

The data was made public on 2016 and can be accessed from the EAGLE website `http://icc.dur.ac.uk/Eagle/database.php`. We mention here the original released paper [17].

2.2 Selection of galaxies alike the Milky Way

The selection of galaxies within the simulation to be taken as analogous of the Milky Way have been a major task during the elaboration of this document. We first take basic physical properties at redshift zero that are similar to the Milky Way, the stellar mass and star formation rate, and then also consider the time since the last significant merger. There is a lot of literature about this topic (e.g. P . J. McMillan (2011) [18]). In this work we have used the stellar mass 6.08 x 10^{10} $M_\odot$ provided by van Licquia et al (2013) [11] and with the associate uncertainty we have let the sample be on a interval from 3.45 x 10^{10} to 8.45 x 10^{10} $M_\odot$.

The star formation rate (SFR) is an important quantity to take into account. For that reason we have classified the galaxies in two different labels active and inactive. We have set the limit of 2 $M_\odot/yr$ being the active (inactive) galaxies above (below) this quantity.

The selection of 2 $M_\odot/yr$ as a limit is based on the behaviour of the sample in the interval of mass based on the figure 1. It is worth noticing that the Milky Way present an inactive SFR based on this selection (SFR 0.5 - 1.5 $M_\odot/yr$ based on the work of Robitaille et al [25]).

Another aspect to take into account is the particular merger story of the Milky Way. From the age of the Milky Way's thin disc stars, it is highly likely that the Milky Way has not suffered a significant merger at least since redshift 1.5 (van Dokkum et al [6]). In this line, we have classified the simulated galaxies by the last time they have suffered a merger in three categories: early, intermediate and late merger based on the last time they suffer a significant merger (defining significant merger as where the accreted galaxy is at least 10% of the total mass of the central galaxy.).

Early merger is referred to these galaxies that suffered its last significant merger prior to redshift 1.5, intermediate between 0.6 and 1.5, and late merger after redshift 0.6. The Milky Way sample has been chosen such that the galaxies contained in it suffered an early merger.

Finally, we have considered the morphology of the galaxies dividing them by disk and non-disk using the morphology data provided by EAGLE.

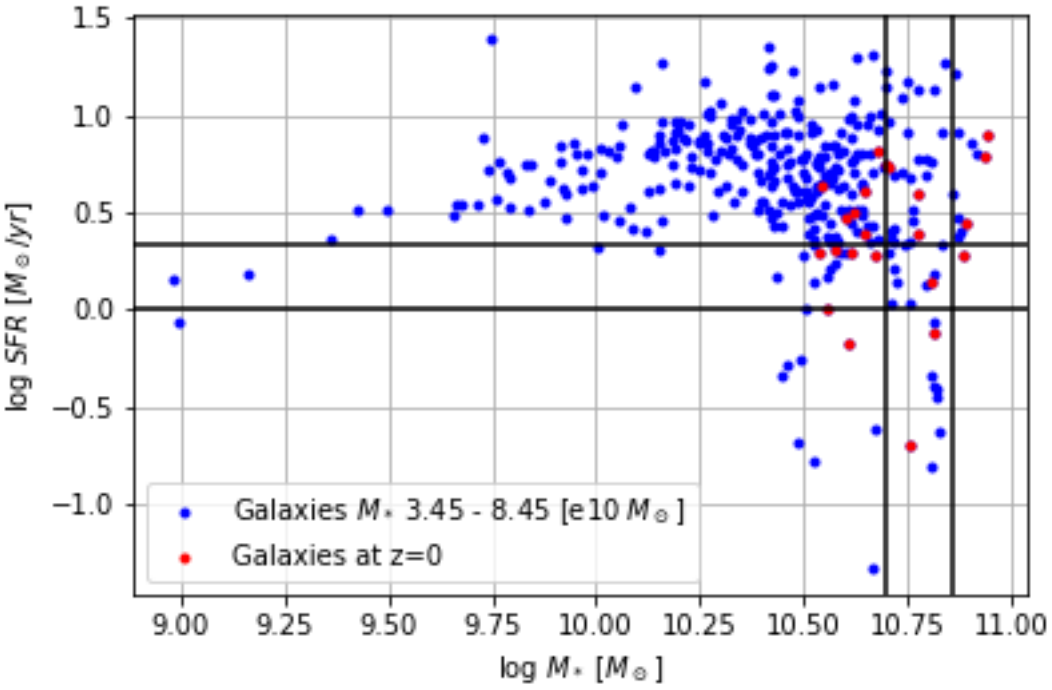

Figure 1: Diagram SFR - Stellar mass. The black lines delimited the SFR and Stellar mass of the Milky Way based on the work of Licquia et al [11] and Robitaille et al [25]. The rest of the points refers to the values found for the simulated galaxies in the interval of mass 3.45 - 8.45 10^{10} x $M_{\odot}$ at different redshifts.

Based on these parameters we have obtained 24 galaxies within the selected stellar mass range of the Milky Way on the simulation. Taking into account the rest of parameters expected for a Milky Way galaxy we have 3 galaxies that fulfill the requirements and another 3 that have a slighter bigger SFR but that have the morphology, early merger and stellar mass expected.

2.3 Tracking of galaxies

Once we have selected our galaxies at z=0, we want to trace them back to their progenitors at high redshift.

It is necessary to distinguish between these two different cases:

1) The tracking of galaxies within simulations

2) The tracking of galaxies observationally.

Both cases require different explanation and below we made a brief discussion about this topic.

2.3.1 Tracking galaxies within a simulation

The ΛCMD cosmology predicts that galaxies form hierarchically, with low mass galaxies merging to form larger galaxies and for this reason it is difficult to follow the history of a galaxy.

However, EAGLE provided a tool that allows us to follow the relation of a galaxy with all its progenitors and give account of all the mergers that occur between snapshots. This kind of diagram is called a merger tree.

We have tracked back our galaxies using this method that, in case of merger, retains as progenitor the most massive galaxy in the previous snapshot. Also, to keep a registry of the significant mergers of the galaxies we have defined as last significant merger the nearest in redshift in which the ratio of mass between the main progenitor and the most massive secondary progenitor is greater than 10 per cent.

2.3.2 Tracking galaxies observationally

Observationally there is no way to directly link galaxies and their progenitors, but several methods exist to attempt to link low redshift galaxies to high redshift galaxies that are analogues of their progenitors. Several studies as van Dokkun et al (2013) [6], Clauwens et al (2016) [4] have used the constant cumulative density method proposed by Loeb & Peables (2003) [12].

This method assumes that the cumulative number density of galaxies remains constant at various redshifts. Essentially, it is assuming that galaxies maintain the same rank ordering of stellar mass at each redshift. This assumption would be satisfied if all galaxies match the average star formation rate-stellar mass relation at all times. however, we know that there is scatter in such relation, meaning that galaxies will change their order (see e.g Guo et al (2013) [8]). Further, merging galaxies will result in galaxies changing their rank order in stellar mass (see e.g Behroozi et al (2013) [1]).

Despite these caveats, the method gives reasonable result according to simulations. Adjustments can be made to include merging process.

3 Code development

The references papers of the EAGLE simulation [5, 17, 28] give a brief discussion of how to read the data and a few examples. However, these programs are not enough to make the vast majority of the work. We provide a discussion of the code development done in this project to create the main plots and draw conclusions. All the programs have been running on different versions of python.

The data is stored in h5py format, with 27 files taken through the evolution of simulation. The particles from a given snapshot have been read using the example given in the public release paper [17] and making minor changes related to the different python's versions. Each particle within the cosmological volume has a GroupNumber, and also a SubgroupNumber if it is a subhalo of a larger galaxy. These are used for identifying the simulated galaxies to which the particles belong and are used extensively in the analysis.

The particles are divided also by kind. There are particles of gas, stars, black holes and dark matter. However only the gas and stars particles have attributed a metallicity that have been used in this work. The rest have been used to check different aspects of the program.

All the coding has been made using python classes. This kind of object are able to save relevant data and build a framework in which different functions can combine to share results. In our calculation we often need to recover data that has been previous calculated and the classes are useful in this sense.

We explore the gas and stars within 15 kpc of the centre of the simulated galaxies, a region that contains the disc.

The metallicity is used represented on the labels as $log(\frac{M}{M_\odot})$ where $M_\odot$ is the solar metallicity. In the followings plots we have selected a value of $M_\odot = 0.012$ based on the recent work by G. Buldgem et al (2017) [2].

3.1 Reading the data of the galaxies

The data have been read running a loop over all the particles on the simulation and selecting those that possess the same group number and subgroup number that the galaxy in question. This allows us to calculate the center of mass ourselves.

Once extracted the particles we need to chose the properties we are going to use later. The different physical variables available depend on the kind of particle.

3.2 Mass center calculation

In the computation we have used as center of the galaxy the center of mass of the stellar particles. Firstly we tried to compute it using the usual formula:

$$\vec{r}_{CM} = \sum_{i=0}^{N} \frac{m_i \vec{r_i}}{m_i} \tag{3.1}$$

with the summatory going through all stars particles in the galaxy.

This method give some problems because the distribution of particles far away from the center is not homogeneous and lead to problems when we made some test as plotting the radial dark matter density.

So instead of it we used an iterative process, as first approximation we took the position of the most massive stars as the galaxy center and then we run the equation 3.1 over the particles that were 15 kpc away from the approximated one and getting a new center of galaxy. This process was repeated using each time a half of the previous length until the mass center converged. In the figure 2 we show the program developed to this issue

This formalism provided good results when we plotted the dark matter density and the rotation curve as a function of the distance to the center. So we used it during all the following discussion.

3.3 Radial and vertical metallicity

The particle database give the coordinates of each particle as an array with three elements, the x, y and z-position with respect to the simulation system. However, when we compute the metallicity we are interested in the radial and vertical metallicity with respect the plane of the disk.

```
def centre_mass(self, gn, sgn):

    centre_aprox = self.stars['coordinates'][np.where(self.stars['mass'] == self.stars['mass'].max())]

    centre  = centre_aprox
    r_gal   = 15            #Typical galaxy lenght

    for i in range(4):

        r       = np.linalg.norm(self.stars['coordinates'] - centre, axis = 1)
        mask    = r <= r_gal / 2**i
        coord   = self.stars['coordinates'][mask]
        mass    = self.stars['mass'][mask]

        centre = sum(np.stack(coord[i]*mass[i] for i in range(len(mass)))) / sum(mass)

    return centre
```

Figure 2: Routine used to calculate the center of mass.

To transform the coordinates provided by EAGLE to the ones referring to the galaxy plane we have picked the angular momentum vector of the galaxy from the EAGLE galaxy database and rotate all the particles of this galaxy to make the angular momentum vector point along the z axis, such that the disc is in the x-y plane.

Once we transform our center of mass and the coordinates of every particle on the galaxy it is possible to subtract both quantities to get the coordinates with respect the mass center and plotting the required properties. This process have been used on the following plots and tested with good results.

For making the metallicity plots we have binned all the particles at intervals of 0.5 or 1 kpc from the center of the galaxy and computing the mean metallicity using the following equation:

$$Z(r) = \frac{\sum_{i=1}^{N} m_i Z_i}{\sum_{i=1}^{N} m_i} \tag{3.2}$$

where the summatory runs over all the particles on the interval and where m and Z represent the mass and the metallicity of each particle.

The metallicity gradient on the disk have been calculated making a linear fit for

the points between 3 and 10 kpc and between 1 and 2 kpc for the radial and vertical respectively.

4 Results

4.1 General properties of the sample

In this section we present the results obtained using the galaxy database that contains general properties of the simulated galaxies in the MW stellar mass range.

Firstly, we noticed that exist a correlation between the morphology of the galaxies and the time elapsed since the last significant merger as we show in figure 3 in which disk galaxies tend to suffer earlier mergers than non-disk galaxies. This result agrees with what is expected by inside-out growth models (Toomre, 1977 [30]).

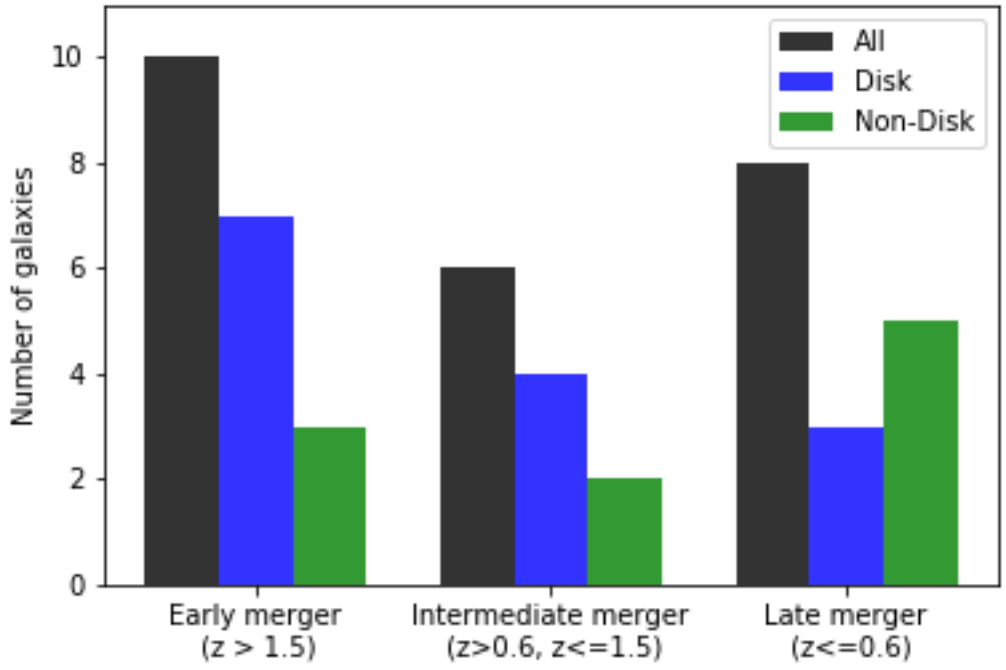

Figure 3: Galaxies divided by morphology and time elapsed since the last merger. There exist a clear correlation in which early merger galaxies tend to show a disk morphology. We have estimated the mean redshift in which disk galaxies have suffered it last merger of about z=1.40 in contrast with the z=0.89 showed by non-disk galaxies

In the figure 4 we plot the evolution of stellar mass with redshift of the sample of galaxies in panel a, whilst in panel b we plot the evolution of the effective radius for the sample of galaxies. We define effective radius as the radius of the sphere that

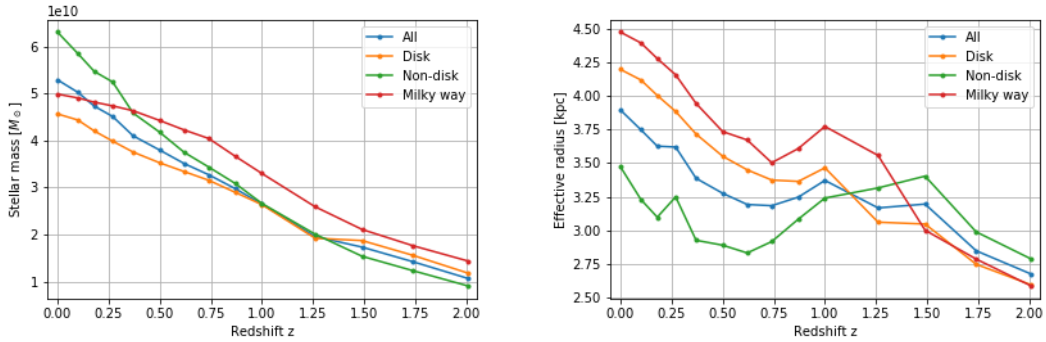

(a) Mass evolution

(b) Radius evolution

Figure 4: Evolution of the mean properties of the sample of galaxies

contains at least 30 % of the total mass of the galaxy from its center than non-disk galaxies. As we can see, disc galaxies have a larger effective radius at the final redshift than non disc galaxies, as one may expect. Also the non disc galaxies actually start with higher effective radius, but they do not grow, whilst disc galaxies are growing inside-out.

In panel a we see a bias within this sample for non disc galaxies to have around 20 % greater stellar mass than disc galaxies. This is likely a result of greater AGN activity as well as mergers, with such mergers being gas poor in more massive galaxies due to the greater effect of AGN. Also is interesting to notice how the Milky Way sample have a behaviour similar to the rest of disk galaxies as we would expect.

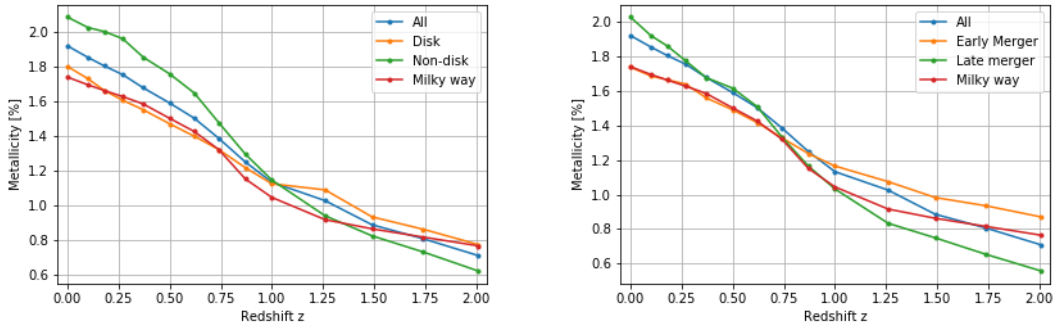

Figure 5: Evolution of the mean metallicity by morph and age. The correlation between age and morphology is even more evident in this case.

Non disc galaxies have greater metallicity than disc galaxies, and also their metallicity evolves more. In panel b it is evident that the galaxies with late merger increase their metallicities, indicating that mergers are involved in metallicity increases as well as changes or morphology.

In figure 5 we plot the evolution of the stellar metallicity of the simulated galaxies between redshift 2 and zero, with the left panel showing the evolution by morphology and the right panel by time elapsed since the last significant merger.

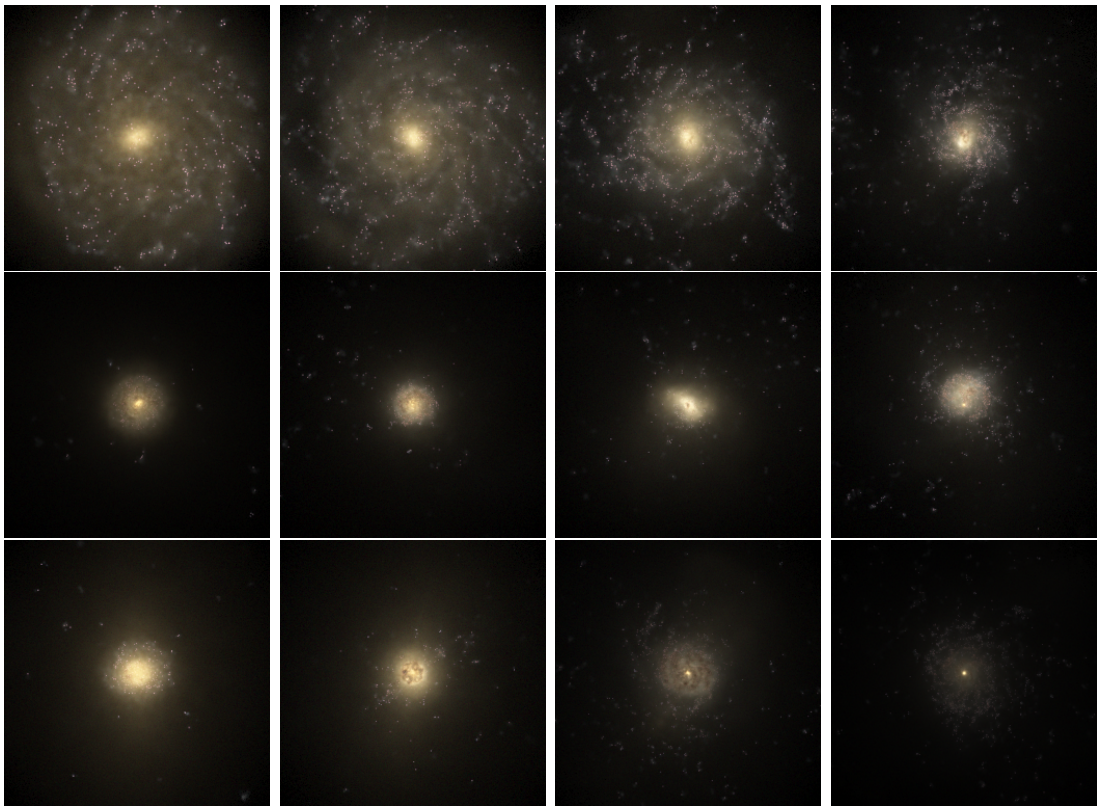

(a) z = 0.0 (b) z = 0.5 (c) z = 1.0 (d) z = 1.5

Figure 6: Morphology evolution of the 3 Milky Way's galaxies from a face view. The width and height of the images correspond to 30 kpc.

From the figure 5 we can extract how the late mergers and non-disk galaxies show about a 0.3 % more metals than the Milky Way's galaxies. This result can be explained arguing that the main difference between the two samples is due to the lack of merger interaction and probably this mergers are partially responsible of causing

growth in the metallicity. The evolution of metallicity during a merger was studied deeply by M. Montouri et al (2010) [20] that predicts also a notable increase of metallicity for merging galaxies.

4.2 Analysis of the evolution in the morphology of galaxies

Here we present different plots of the evolution of the morphology of the galaxies on the sample. The figures don't represent the total sample but instead show a representative sample.

In figure 6 are plotted the evolution of the Milky Way's galaxies. The evolution display the expected by an inside-out model in which the growth is due to the capture of gas particles on the external part of the galaxy, this produces an increase in the effective radius of the galaxy as shown by R. Roskar et al (2008) [26] in his study about inside-out model and that is consistent with our previous result in figure 4.

This contrast with the observed evolution in galaxies that have suffer mergers as the ones showed in figure 7 in which the mergers destroy discs and disrupt their growth. Further, significant amounts of mass are added during the merger rather than through gas accretion.

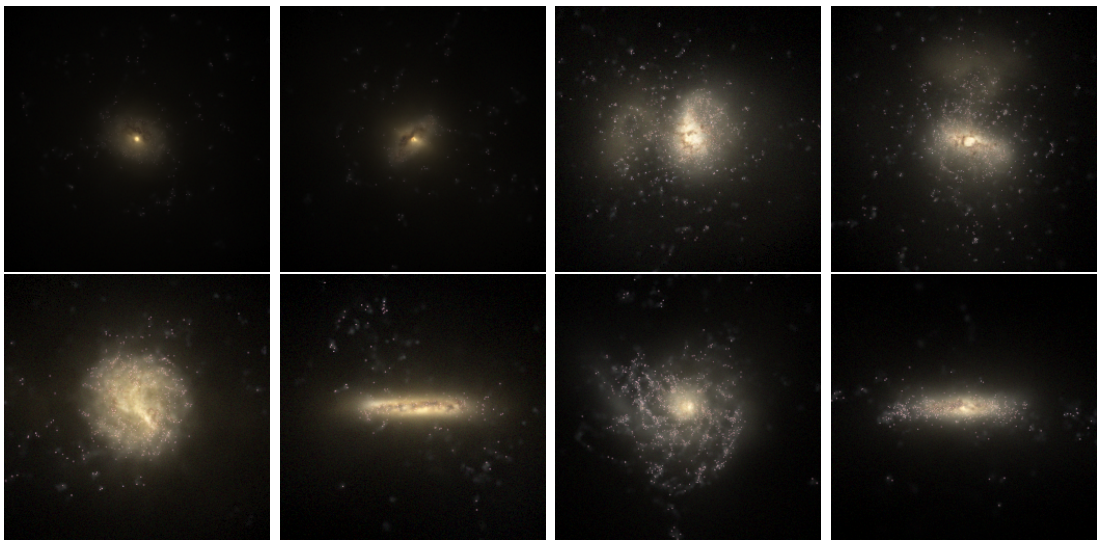

(a) Face (z=0) (b) Edge (z=0) (c) Face (z=1.5) (d) Edge (z=1.5)

Figure 7: Evolution on the morphology of different galaxies within the sample

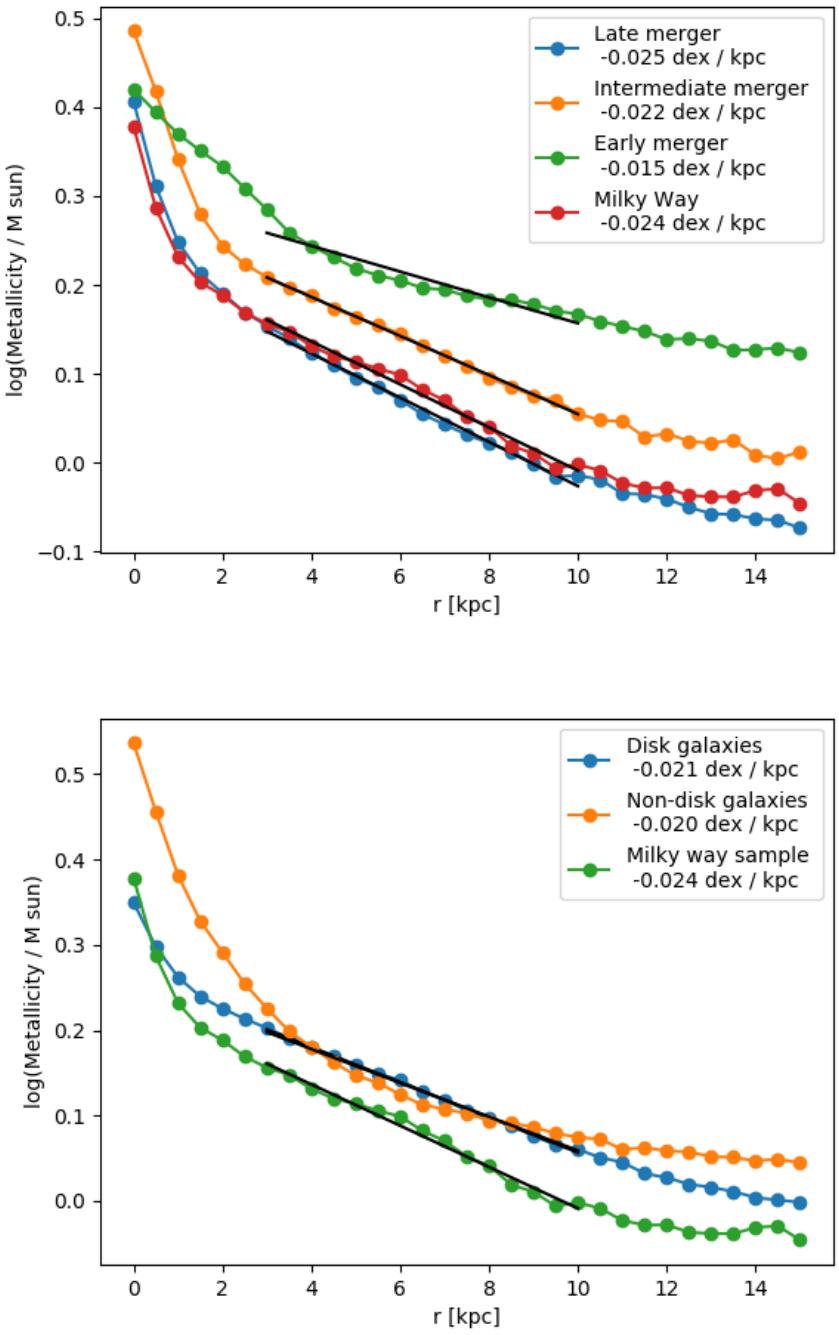

Figure 8: Radial metallicity at redshift 0. We show the radial metallicity gradients for various populations. The top panel shows the total, late, intermediate and early merger samples while the bottom one the discs, non discs, and MW samples.

4.3 Analysis of the metallicity

4.3.1 Radial metallicity at redshift 0

The radial metallicity by age and by morphology is plotted in figure 8. On the top panel it is plotted the metallicity attending to the time elapsed since the last significant merger referring the blue, orange and green lines to late, intermediate and early merger. The red line is reserved for the Milky Way sample. The bottom panel show a classification by morphology with the blue, orange and green lines referring to disk, non disk and MW sample respectively.

In this case the Milky Way sample differs significantly from the rest of disk galaxies so morphology can't be treated as a parameter able to identify Milky Way galaxies from a metallicity perspective.

However, the MW and the early merger sample show a similar behaviour. It is interesting to notice that also exist a correlation between the gradient of the galaxies and the time since the last merger tending recent galaxies to show flatter gradients. Miranda et al (2015) [19] shows a similar behaviour of the gradient for a population of MW galaxies on various hydrodinamical simulations.

The last result can be explained considering the role of the merger in the distribution of metallicity. One could expect that when a galaxy suffer a merger process its radial metallicity distribution changes notably suffering an increase of the metallicity on its outer part producing a flatter gradient. It has been shown that this gradient increase with the time elapsed since the last merger so we affirm that there must exist some mechanism able to redistribute the metallicity along the galaxy.

In recent times this process of flattering of galaxies after merger have been found in different hydrodinamical simulations (Ma et al (2015) [14]).

4.3.2 Evolution of the radial metallicity

In the figure 9 we plot the radial metallicity at redshift 1.5 attending to its properties at redshift 0. The plot is quite similar to the one showed for the metallicity at redshift 0.

The metallicity bumps that appear at 2 and 9 kpc can be attributed to recent merger process in galaxies that haven't time to redistribute the metals.

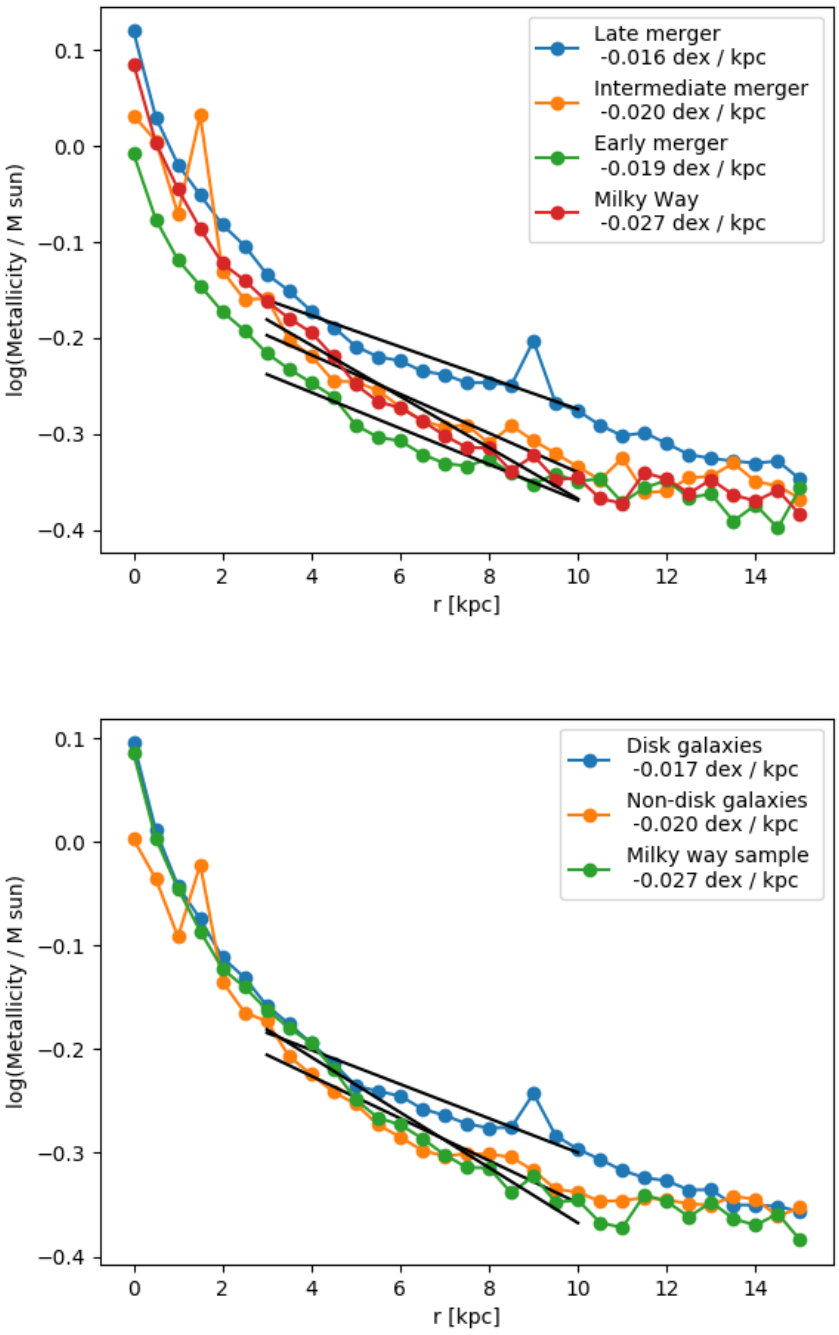

Figure 9: Radial metallicity at redshift 1.5. We plot the radial metallicity for various populations. In the top panel we plot the different samples classified by time elapsed since the last significant merger while in the bottom they are classified by morphology.

It is interesting to notice how all the sample posses a similar behaviour independently of its properties at redshift 0 which indicates that the fundamental parameter that characterise the metallicity gradient is the time elapsed since the last merger.

Furthermore, it has is clear that under the classification at redshift 0 the calculation of the gradient by a linear fit between 3 and 10 kpc is not a robust measure of the metallicity gradient, and should be treated with caution.

Finally, in the figure 10 we show the evolution of the MW sample. As expected from the evolution of the mean metallicity plotted above we have a great increase in the total metallicity due the continuous formation of metal in stars.

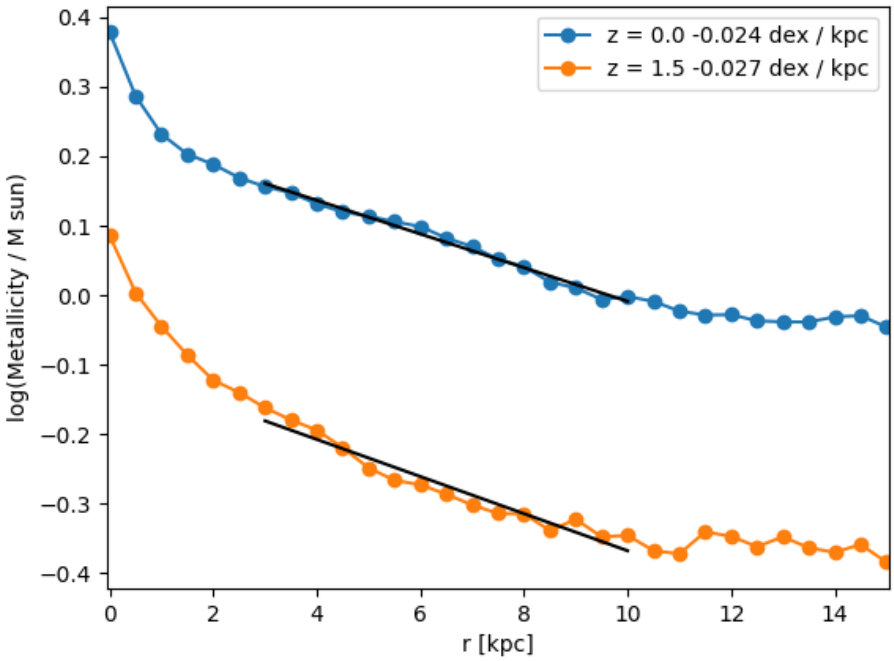

Figure 10: Evolution of the radial metallicity for the Milky Way sample

The gradient keeps almost constant in both redshifts and it is flattened at redshift 0 compared to redshift 1.5. We have shown that after merger interaction the galaxy gradient gets flatter so we would expect that the gradient showed in figure 10 for a sample that haven't suffered a significant merger represent an upper limit to the radial gradient of MW galaxies in which the vast majority of the metals have been

distributed along the galaxy.

4.3.3 Study of the vertical metallicity

The vertical metallicity gradient have been used in classic works as a extremely effective way to distinguish the thin and thin disk of galaxies (See Marsakov and Borkova (2006) [16]). In the figure 11 we have plotted the vertical metallicity at redshift 0 and 1.5 by morphology.

As can be seen the EAGLE simulation is not able to distinguish between thin and thick disk. This can be explained arguing that different work that studied metallicity gradient in the Milky Way using different species (mainly Fe/H and Mg/H) shows that the length of transition between thin and thick disk is about 0.3 - 0.4 kpc.

However, the softening length of the intermediate resolution of EAGLE simulation is about 0.3 kpc. Usually the total resolution of a simulation is took as 3 times this softening length (C. Power et al (2003) [24]) which indicates a resolution of the EAGLE simulation of about 1 kpc, not enough to distinguish thin and thick disk.

In figure 11 we plot the sample divided by morphology. In the top panel we plot the sample at redshift 0 while in the bottom it is at z=1.5. In both cases we have used the blue, orange and green colour to denote the disk, non-disk and MW sample respectively.

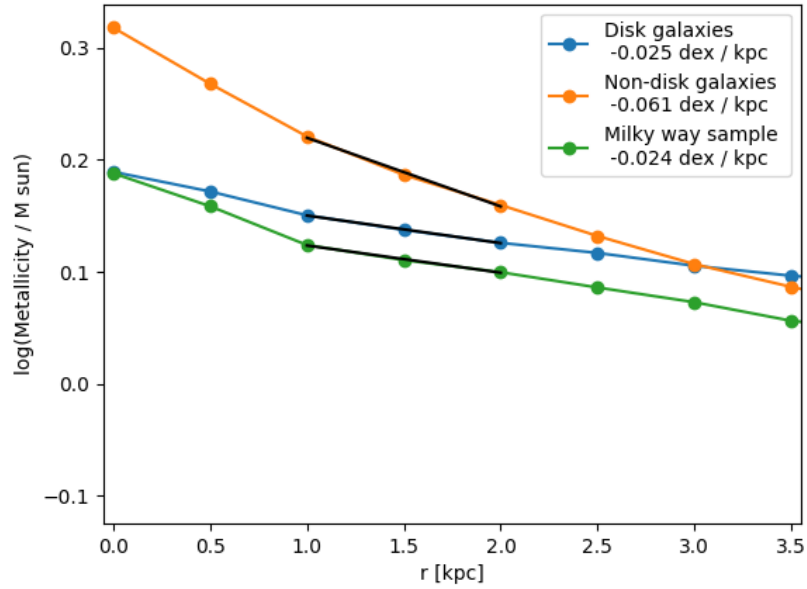

(a) z = 0

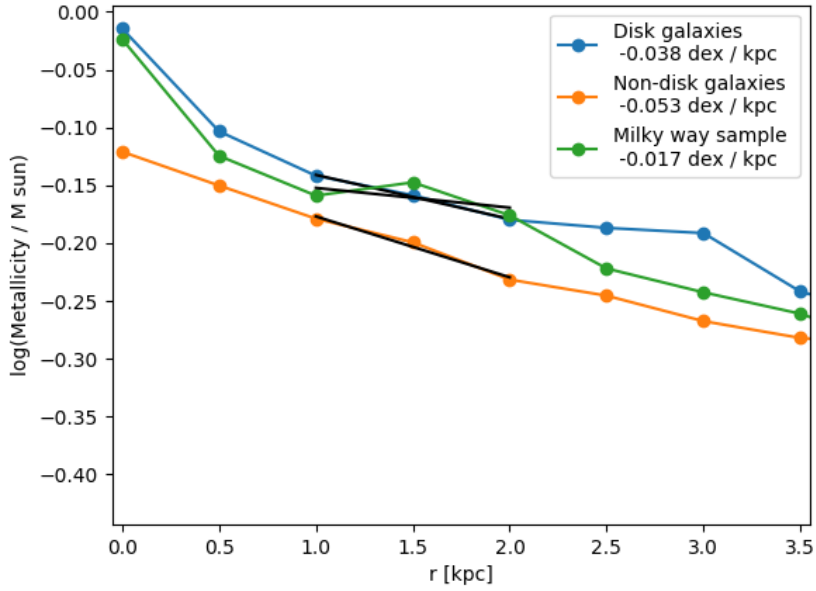

(b) z = 1.5

Figure 11: Vertical metallicity.

5 Conclusions

In this study we have explored the evolution of metallicity gradients in Milky Way mass galaxies within the EAGLE simulation suite. We have compared the radial trends and other general properties of disk and non disk galaxies with its expected growth model. The main findings are:

- There exist a clear correlation between the morphology of galaxies and the last time they have suffered a merger (Disk galaxies tend to be older than non-disk). Disk galaxies also show a bigger effective radius but a smaller stellar mass and metallicity than the rest of the sample.

- The merger interaction is thus seen to be responsible for morphology in the EAGLE simulations, consistent with many studies on the merging process (e.g A. Toomre (1977) [30], M. Montouri (2010) [20]). However we let open the question is his main results is extrapolable to hydrodinamical simulations as the EAGLE one.

- Analysing the evolution on the morphology and the effective radius of the Milky Way and the early merger sample we affirm that the evolution of this kind of galaxies can be explained using an inside-out growth model, with a clear increase in effective radius in the galaxies so long as mergers are not present.

- The radial metallicity of Milky Way sample correspond to the expected for a galaxy that haven't suffered mergers at least since z=1.5. We support the main conclusion presented in van Dokkum et al (2013) [6] that assign a similar merger history to the Milky Way.

- The radial metallicity gradient tends to be smaller in late merging galaxies. We observe an increase in the metallicity gradient during the evolution of galaxies that don't suffer merger process. This is consistent with the notion that mergers are able to redistribute metals of galaxies.

  The recent work of X. Ma et al [14] found analogous result in other cosmological simulations.

- The metallicity at redshift 1.5 looks similar on all the samples considered which indicates again that the main parameter to explain the radial distribution is the time elapsed since the last merger.

- EAGLE simulations are unable to distinguish between the thin and thick disk on galaxies by its vertical metallicity. This result is expected as the thin disk in MW galaxies have an scale height of about 0.3 - 0.4 kpc while the resolution of the softening length should be taken around 1 - 1.5 kpc.

  On the other hand, the thick disk is well defined and we have found for disk galaxies a gradient of 0.3 dex/kpc in this set of simulated galaxies.

The above conclusion is a great example of how a qualitative analysis of the chemical evolution on galaxies is able to provide several insights to describe the formation of galaxies.

The confirmation of an inside-out growth for late merger galaxies and the exact role of merger interaction in the distribution of radial and vertical metallicity are two main problems that deserve a further investigation.

It would be interesting also to made a more complete analysis of the vertical metallicity in a high resolution hydrodinamical simulation to prove if this kind of simulation are able to distinguish the thick from the thin disk.

References

[1] P. S. Behroozi and R. H. Wechsler, 2013, ApJ.

[2] G. Buldgen, S. J, A, J, Salmon, A. Noels, R. Scuflaire, M. A. Dupret and D. R. Resae, MNRAS, 000, 1 - 15 , 2017.

[3] R. Carrera , C. Gallart, A. Aparicio et al. 2008, AJ, 136, 1039.

[4] B. Clauwens, M. Franx, J. Schaye, MNRAS, 000, 1 - 5, 2016.

[5] R. A. Crain, H. Schaye, R. G. Bower, M. Furlong, M. Schaller, T. Theuns et al. MNRAS, 450:19371961, June 2015.

[6] P. G. van Dokkum, J. Leja, E. J. Nelson, S. Patel, R. E. Skelton, I. Momcheva et al, 2013, APJL, 771, L35.

[7] S. M. Fall and G. Efstathiou, 1980, MNRAS, 193, 189-206.

[8] K. Guo, X. Z. Zheng and H. Fu, ApJ, 2013, 778:23.

[9] D. Kawata, C. Allende, C. B. Brook, L. Casagrande, I. Ciuca, B. K. Gibson, R. J. J. Grand, M. R. Hayden and Jason A. S. Hunt, 2017, MNRAS, 473, 867 - 878.

[10] L.J. Kewley, D. Rupke, H. Jabran Zahid, M. J. Geller and E. J. Barton, 2010, ApJ, 721, L48.

[11] T. C. Licquia, J. A. Newman, 2015, ApJ.

[12] A. Loeb and P. J. E. Peebles, 2003, AAS, 528:29-34.

[13] R. E. Luke and D. L. Lambert, 2011, AAS, 142, 4.

[14] X. Ma, P. F. Hopkins, R. Feldmann, P. Torrey et al, 2016, MNRAS, 000, 1-15.

[15] J. T. Mackereth, J. Bovy, R. P. Schiavom, G. Zasowski, K. Cunha et al, 2017, MNRAS, 000, 1 - 21.

[16] V. A. Marsakov and T. V. Borkova, 2006, Astron. Lett., 32, 376.

[17] S. McAlpine, J. C. Helly, M. Schaller, J. W. Trayford, Y. Qu, M. Furlong et al, 15:7289, April 2016.

[18] P. J. McMillan, 2011, MNRAS, 000, 00-00.

[19] M. S. Miranda, K. Pilkington, B. K. Gibson, C. B. Brook, P. Sánchez-Blázquez et al, 2015, AA.

[20] M. Montuori, P. Di Matteo, M. F. Lehnert, F. Combers and B. Semelin, 2010, AA, 518, A56.

[21] M. Ness, K. Freeman, 2015, PASA, doi:10.1017.

[22] S. Pedicelli, G. Bono, B. Lemasle, P. Franois, M. Groenewegen et al, 2009, AA.

[23] K. Pilkington, C. G. Few, B. K. Gibson, F. Calura, L. Michel-Dansac, R. J. Thacker, M. Mollá, F. Matteucci, A. Rahimi, D. Kawata, C. Kobayashi, C. B. Brook, G. S. Stinson, H. M. P. Cpuchman, J. Bailin and J. Wadsley, 2012, AA, 540, A56.

[24] C. Power, J. F. Navarro, A. Jenkis, C. S. Frenk, S. D. M. White, V. Springel, J. Stadel and T. Quinn, 2003, MNRAS, 338, 14 - 34.

[25] T. P. Robitaille and B. A. Whitney, arXiv:1001.3672v1, January, 2010.

[26] R. Roskar, V. P. Debattista, G. S. Stinson, T. R. Quinn, T. Kaufmann and J. Wadsley, 2008, AJ, 675: L65-L68.

[27] P. Sánchez-Blázquez, P. Ocvirk, B. K. Gibson, I. Pérez and R. F. Peletier, 2011, MNRAS, 415, 709.

[28] J. Schaye, R. A. Crain, R. G. Bower, M. Furlong, M. Schaller, T. Theuns et al, 2015, MNRAS, 446: 521554.

[29] P. A. Shaver, R. X. McGee, L. M. Newton, A. C. Danks and S. R. Pottasch, 1983, MNRAS, 204, 53.

[30] A. Toomre, 1977, ARAA, Vol. 15:437-478.